



Combined SMAP/SMOS Thin Sea Ice Thickness Retrieval

Cătălin Pațilea¹, Georg Heygster¹, Marcus Huntemann^{2,1}, and Gunnar Spreen¹

¹Institute of Environmental Physics, University of Bremen, Bremen, Germany

²Alfred Wegener Institute, Bremerhaven, Germany

Correspondence to: Cătălin Pațilea (cpatilea@iup.physik.uni-bremen.de)

Abstract. The spaceborne passive microwave sensors Soil Moisture Ocean Salinity (SMOS) and Soil Moisture Active Passive (SMAP) provide brightness temperature data at L-band (1.4 GHz). At this low frequency the atmosphere is close to transparent and in polar regions the thickness of thin sea ice can be derived. SMOS data covers a large incidence angle range whereas SMAP observes at a fixed 40° incidence angle which makes thin sea ice thickness retrieval more stable as incidence angle effects do not have to be taken into account. Here we transfer a retrieval algorithm for thickness of thin sea ice (up to 50 cm) from SMOS data at 40° to 50° incidence angle to the fixed incidence angle of SMAP. Now the SMOS brightness temperatures (TBs) at a given incidence angle are estimated using empirical fit functions. SMAP TBs are calibrated to SMOS for providing a merged SMOS/SMAP Sea Ice Thickness product.

1 Introduction

10 Sea ice is an important climate parameter and accurate knowledge of sea ice properties are needed for improved climate modeling and prediction. The thickness of the ice determines resistance against the deforming forces of wind and ocean currents. Even a thin layer of sea ice inhibits evaporation, reduces heat and gas exchange between ocean and atmosphere and increases the albedo. It provides a solid surface for snow to deposit, which further reduces heat exchange and increases albedo.

The Soil Moisture Ocean Salinity (SMOS) satellite was launched by ESA in November 2009. It is a synthetic aperture passive 15 microwave radiometer working at L-band (1.4 GHz). Modeling and observations showed that at this frequency radiation varies with ice thickness up to 0.5 meters (Kaleschke et al., 2010, 2012). The atmosphere has little influence on the radiation at L-band as both absorption and scattering are small. These aspects make SMOS a candidate for thickness retrieval of thin sea ice. Two retrieval algorithms have been developed for SMOS, one using the intensity at incidence angles between 0° and 40° (Tian-Kunze et al., 2014) and one using intensity and polarization difference at incidence angles between 40° and 50° (Huntemann et al., 2014). In 2015 the Soil Moisture Active Passive (SMAP) satellite was launched by NASA. It has two sensors onboard, 25 an L-band radiometer and a radar.

Here we present a mixed Sea Ice Thickness (SIT) dataset combining data of the two sensors by calibrating the SMAP brightness temperatures (TBs) to those of SMOS (Sect. 4). In addition, the SIT retrieval from Huntemann et al. (2014) is adapted to the new version 6.20 of the SMOS Level 1C data and it will be used as a reference for all other comparisons 25 (Sect. 3.1). This is combined with the introduction of a fit function for the dependence of horizontal and vertical brightness temperatures (from now on referred as TB_h and TB_v , respectively) on the incidence angle (Sect. 3.2). It is used for Radio



Frequency Interference (RFI) filtering and for SIT retrieval at a fixed incidence angle. This is also a required step for the SMOS and SMAP merged product to combine the observations of the two sensors at a common incidence angle.

2 SMOS and SMAP data sources

The SMOS satellite has 69 receivers on three arms measuring radiances at 1.4 GHz (Kerr et al., 2001). One complete set of data from the aperture synthesis process done each 1.2 seconds is called a snapshot. For this investigation the SMOS Level 1C sea data gridded on the icosahedron Snyder equal area (ISEA) 4H9 grid (Sahr et al., 2003) is used. Its resolution is 15 km while the SMOS footprint size varies with incidence angle from approximately 30 km×30 km at nadir to 90 km×30 km at 65° (Castro, 2008). The Level 1C data is provided within 24 h of acquisition.

In full polarization mode all four Stokes parameters are measured. Data is recorded in the reference plane of the antenna as T_X , T_Y , T_3 and T_4 , and are converted to TB_h , TB_v , TB_3 and TB_4 in the Earth surface plane (Zine et al., 2008) using

$$\begin{bmatrix} T_X \\ T_Y \\ T_3 \\ T_4 \end{bmatrix} = \begin{bmatrix} \cos^2(\alpha) & \sin^2(\alpha) & -\cos(\alpha)\sin(\alpha) & 0 \\ \sin^2(\alpha) & \cos^2(\alpha) & \cos(\alpha)\sin(\alpha) & 0 \\ \sin(2\alpha) & -\sin(2\alpha) & \cos(2\alpha) & 0 \\ 0 & 0 & 0 & 1 \end{bmatrix} \begin{bmatrix} TB_h \\ TB_v \\ TB_3 \\ TB_4 \end{bmatrix}, \quad (1)$$

where $\alpha = \alpha_{gr} + \omega_{Fr}$, α_{gr} is the the georotation angle and ω_{Fr} is the Faraday rotation angle. Within a snapshot just one or two of the Stokes parameters are measured at the same time. The missing values required for the conversion are interpolated from neighboring snapshots within a 2.5 s range and with a maximum incidence angle difference between the measurements of 0.5°.

The SMOS L1C data version 6.20 has been available since 5 May 2015 operationally and older acquisitions were reprocessed. It adds better RFI flagging and it improves the long-term and seasonal stability of the measurements. At the same time it introduces a warm bias in the brightness temperatures of approximately 1.4 K relative to the previous version 5.05 over ocean while Antarctica and land have a bias above 2 K which is closer to modeled and ground based measurements (SMOS Calibration team and Expert Support Laboratory Level 1, 2015). The new data version also reduces the difference in brightness temperature between ascending and descending overflights over ocean at low latitudes. Changes at high latitudes were not documented. Before, the difference varied considerably with time and latitude due to thermal variations in the instrument.

SMAP started providing data starting in April 2015. It is positioned on a quasi-polar sun-synchronous orbit with ascending equator crossing time at 6 pm, while SMOS has a equator crossing time at 6 am. SMAP carries a conically scanning radiometer with a fixed incidence angle of 40° which leads to a narrower swath and decreases the area covered at the pole compared to SMOS. In this study the SMAP Level 1B data is used which contain time ordered ungridded top of the atmosphere brightness temperatures. The data is provided with a latency of about 12 h. The SMAP footprint is approximately 36×47 km.

The frequency bands of both SMOS and SMAP are located in a restricted band (1.400-1.427 GHz) reserved for passive radioastronomical use. Nevertheless there are surfaced based artificial sources causing RFI. The image reconstruction process required to obtain the SMOS TBs includes an inverse Fourier transform. Therefore, not only the grid cells that contain the RFI



source are affected, but the whole snapshot can be contaminated resulting in high or even negative brightness temperatures. Since in nature brightness temperature will not exceed 300 K over the polar ocean, a simple filter for the RFI is to eliminate the whole snapshot which contains at least one TB exceeding this threshold. This filter is used in sea ice thickness retrieval algorithm presented in Huntemann et al. (2014). An alternative approach for filtering RFI has been shown in Huntemann and
5 Heygster (2015) where incidence angle binning is used, resulting in a higher preservation of data and fewer gaps on the grid. Since SMAP contains onboard hardware for detection and filtering of RFI and neighbouring pixels are unaffected by a RFI source, no additional filtering is required for the SMAP Level 1B data.

3 Sea ice thickness retrieval using a fit function

Due to the new SMOS data version 6.20 used here compared to version 5.05 used in Huntemann et al. (2014), a retraining
10 of the SMOS thin ice thickness is necessary. First, in Sect. 3.1 we use the method presented in Huntemann et al. (2014) just using the newer data version 6.20. This involves averaging the brightness temperatures between 40 and 50° incidence angle. In Section 3.3 we present an improved ice thickness retrieval based on a fitting function (Sect. 3.2) through the full incidence angle range. This will provide more stable brightness temperatures and is necessary for a consistently combined SMOS and SMAP ice thickness retrieval.

15 3.1 SMOS retrieval retraining

Three SMOS grid cells in the Kara and Barents Sea were used for training over a period of three months (1 October - 26
December 2010) with sea ice thickness data obtained using the relation with the Cumulated Freezing Degree Days (CFDD)
based on NCEP temperature data (Huntemann et al., 2014). CFDD is the daily average temperature below -1.8° (freezing point
of sea water), integrated over the time with sub freezing temperatures (Bilello, 1961). The brightness temperatures are averaged
20 daily over the incidence angle range between 40° to 50°. The resulting sea ice thickness retrieval curve is:

$$\begin{aligned} I_{abc}(x) &= a - (a - b) \cdot \exp(-x/c), \\ Q_{abcd}(x) &= (a - b) \cdot \exp(-(x/c)^d) + b, \end{aligned} \tag{2}$$

where a, b, c and d represent the curve parameters (Table 1), x is the sea ice thickness while I and Q are the brightness temperature intensity and polarization difference, respectively.

Figure 1 shows the intensity (left) for 29 October 2010 using daily mean TBs for each grid cell. The data has been regridded
25 to the NSIDC polar stereographic projection with a resolution of 12.5 km. The original validated retrieval was trained with the old data version hence it is used as a reference here. The warm bias of the new data is seen in the difference plot (Fig. 1 right) both over ocean area and sea ice. In regions of high contrast like the ice edge or coastlines, the old data version 5.05 tended to produce spillover effects. They are reduced in the new data version 6.20 with improved image reconstruction techniques (SMOS Calibration team and Expert Support Laboratory Level 1, 2015).



Figure 2 shows the initial sea ice thickness retrieval curve for data version 5.05 (black) and the retrained curve using the 6.20 data version (blue). The new curve has about 1.7 K higher value at zero SIT for intensity and polarization difference. The difference increases up to 3 K at 50 cm SIT.

The algorithm trained with SMOS data version 5.05 has been compared with that trained with version 6.20 for the period 1 October to 26 December 2010 considering sea ice thickness starting from 1 cm to 50 cm. The bias of the new retrieval is -0.22 cm while the RMSD is 1.35 cm. From a total of 5.1 million data points, 97% have at most 3 cm difference. The bias and standard deviation are under ± 1 cm and 2 cm, respectively, for ice thicknesses below 25 cm and it increases to +4 cm and 11 cm, respectively for 50 cm thickness.

Also the two algorithms have been compared as above with the difference that both of them have as input just the new data version. This allows to estimate the error introduced by the usage of the original retrieval (Huntemann et al., 2014) with the new data. The bias between the retrained retrieval and the original one is 0.33 cm with 99% of the data having a difference of 3 cm or less, while the RMSD is 0.91 cm. This means, although it is recommended to use the algorithm adapted for the new data version, the error is below 1 cm thickness on average for under 51 cm SIT data if processed with the old algorithm given above.

3.2 SMOS TBs fit characteristics

In the previous section we showed that the SIT retrieval is consistent with the validated algorithm while using the new data version. In all of the next sections the SMOS Level 1C 6.20 data version will be used, and when making reference to the original daily mean sea ice thickness retrieval, the retrained 6.20 data version algorithm from Sect. 3.1 will be utilized. In each grid cell, the number of data points and the covered incidence angle range are highly variable due to the orbit characteristics, the large incidence angle range of 0° to 65° , and the complex distribution of incidence angle within a SMOS snapshot. Grid cells located near the center of the swath will cover a large incidence angle range. Closer to the swath edges the range is reduced due to lack of coverage of the low incidence angles. Moreover, the RFI filtering removes data and can create a local bias in the average incidence angle. Within one grid cell, this may shift the average incidence angle of the ensemble of observations between 40° and 50° away from the assumed average of 45° , and the average brightness temperatures and SIT values retrieved from them will be corrupted by the corresponding shifts. This error can be avoided by fitting a curve to the angular dependent brightness temperatures, allowing for a fixed incidence angle to be used for retrieval.

Here we propose as a solution a modified version of the fit functions described in Zhao et al. (2015). The fit is applied separately to each polarization, horizontal and vertical, for each grid cell using daily observations. An initial filtering of RFI is done by removing observation which were flagged in Level 1C data for either being affected by tails of point source RFI or for indicating RFI by the system temperature standard deviation exceeding the expected trend (Indra Sistemas S.A., 2015).

The fit is done iteratively with a maximum of five steps. At each step, the 20% of the observations with the highest absolute difference from the fit are removed if the RMSD of the fit is higher than 5 K or if the RMSD fit difference between successive iterations exceeds 1 K. For each step the parameter C (Eq. 3) is determined by averaging the sum of the polarizations for each observation. Due to asymmetric change in TB between horizontal and vertical polarization at higher incidence angles, only



grid cells with at least one observation under 40° are considered. This increases the stability of the fit since $C/2$ represents the intensity at nadir. The 40° threshold was selected due to increased asymmetry between vertical and horizontal brightness temperatures at higher incidence angles which will generate a bias in the computation of the C parameter. The other five fit parameters a_h, b_h, a_v, b_v and d_v in the fit functions

$$\begin{aligned} TB_h(\theta) &= a_h \cdot \theta^2 + \frac{C}{2} \cdot [b_h \cdot \sin^2(\theta) + \cos^2(\theta)] \\ TB_v(\theta) &= a_v \cdot \theta^2 + \frac{C}{2} \cdot [b_v \cdot \sin^2(d_v \cdot \theta) + \cos^2(d_v \cdot \theta)]. \end{aligned} \quad (3)$$

are determined by a least squares procedure. The Brewster angle effect on influencing the vertically polarized TBs is represented by the additional parameter d_v .

The fit function is not optimised for extrapolation of the covered incidence angle range. Incidence angles not covered by the observations will have high uncertainty. To avoid extrapolation, only grid cells with the incidence angle range of observations that covers the wanted angle, e.g. 45° , are used for the retrieval.

3.3 Sea ice thickness retrieval training using fitted data

The retrieval algorithm has been retrained as described in Sect. 3.1 but now using as input brightness temperatures obtained through the fit process presented in Sect. 3.2 using a nominal incidence angle of 45° . The resulting retrieval curve (Fig. 2 green) has 1.3 K higher polarization difference at 0 cm ice thickness than the algorithm trained with the daily mean data (blue). The difference decreases to 0.1 K at 20 cm thickness and increases to approximately 0.5 K at 50 cm. This comes from variability in mean incidence angle. The daily averaged observations have an incidence angle bias of -0.5° (with single differences as high as -2.5°) relative to the assumed 45° one. The smaller incidence angle will result in a smaller polarization difference since this decreases when approaching nadir. The ocean and thin sea ice have low intensities and high polarization difference. As sea ice gets thicker, the intensity increases and the polarization difference decreases. For the same incidence angle bias at higher thicknesses the polarization difference error will be smaller. The intensity values for the two curves at the same sea ice thickness are nearly the same. The difference between these two curves is small compared to the difference to the retrieval curve for the SMOS 5.05 data version (Fig. 2 black).

Figure 4 shows the retrieved sea ice thickness using the daily mean method (left) presented in Sect. 3.1 and the retrained retrieval curve at nominal 45° incidence angle (centre) based on the fitted brightness temperatures for 29 October 2010. Due to the requirement for the fit computation to have observation below 40° (Sect. 3.2), many grid cells in the central Arctic are not covered anymore. The decrease is around 1° in latitude, corresponding to approximately 1000 grid cells. This area is mostly covered by multiyear ice with thickness higher than 50 cm thus not being the focus of the retrieval. On the other hand for many ocean areas which formerly were excluded by the RFI filtering (grey in Fig. 4 left) now data is available, e.g. around Iceland, Eastern Greenland and Vladivostok. At the same time in the area of the Hudson Bay there is a 30% decrease in the area covered due to the high uncertainty of the fit.

Figure 3, for 29 October 2010, shows the difference between the daily mean and the fitted brightness temperatures retrievals for pixels with SIT smaller or equal to 50 cm and at least one of the retrievals returning a non-zero value. For 90% of the grid



points the difference is less than 3 cm which is below the estimated retrieval error of 30% of SIT. The daily mean retrieval has a positive bias of 0.69 cm. The highest differences appear north of Alaska with values up to 10 cm (Fig. 4 right). This is a result of a biased distribution of the incidence angles, resulting in a large number of grid points having under 45° mean incidence angle. This decreases the polarization difference dragging the resulting SIT to higher values. Overall the RMSD is 2.2 cm which is within the error margin of the retrieval.

4 Sea ice thickness retrieval using SMAP data

This section adapts the SMOS SIT algorithm to observations of SMAP. In order to apply the SIT retrieval calibrated with SMOS data also to those of SMAP, first the brightness temperatures of both sensors have to be inter-calibrated (Sec. 4.1). In Section 4.2 the resulting inter-calibrated brightness temperatures are mixed and used for generating a combined SMOS/SMAP sea ice thickness dataset.

4.1 SMAP TBs calibration using 40° SMOS fit data

The first step is to retrain the SMOS retrieval as in Sect. 3.3 using the nominal incidence angle of 40°, which is the fixed incidence angle of SMAP. The resulting SIT retrieval curve is shown in red in Fig. 2. As expected, the lower incidence angle results in a lower polarization difference especially for thin ice and reduces the usable polarization difference range for the retrieval from 22-54 K to 17-43 K.

A procedure to convert between SMOS and SMAP TBs over land was previously suggested in Lannoy et al. (2015). It uses a radiative transfer model and auxiliary data for taking in account atmospheric and galactic contributions for SMOS. For interpolation of SMOS TBs to 40° incidence angle it fits a quadratic function to the angular dependent SMOS TBs.

For this study, in order to use SMAP data for SIT retrieval, we perform a linear regression of SMAP brightness temperatures to bring them to an equivalent 40° SMOS incidence angle. For the calibration we use the period 1 October to 31 December 2015, which covers the freeze-up in the Arctic observed by both sensors. A similar calibration of SMAP to SMOS TBs was presented previously in Huntemann et al. (2016). This used gridded SMAP Level 1C TB product and a two step linear regression for the calibration of SMAP TBs to daily mean SMOS TBs.

The SMAP TBh and TBv data is gridded daily on the SMOS used ISEA 4H9 grid using a Gaussian resampling with a cutoff distance from the grid cell center of 20 km and Full Width Half Maximum (FWHM) range of 40 km. Only grid cells located more than 100 km away from the coast are considered to minimise the land contamination effect.

The resulting linear regression parameters are presented in Table 2. One source for the difference between the brightness temperatures of the two sensors is that SMAP Level 1B includes corrections for galactic contamination and sun specular reflection which is not the case in the SMOS data.

For a daily sea ice thickness retrieval, based on SMAP brightness temperatures only, both horizontal and vertical, are first adjusted to the SMOS brightness temperature using the linear regression parameters. Then they are gridded into a 12.5 km resolution NSIDC polar stereographic grid using a Gaussian weighting for the distance with a cutoff from the grid cell center



of 15 km and FWHM range of 40 km. For 11 October 2015 (not shown) the differences in sea ice thickness between SMOS fitted TBs retrieval and SMAP retrieval are small. The RMSD of the SIT between the two retrievals for thicknesses below 51 cm is 2.0 cm with 0.4 cm positive bias for the SMOS SIT.

4.2 SMOS/SMAP combined sea ice thickness retrieval

5 Because of the small differences of the retrievals from the two sensors, combined maps are produced using both of them. The daily mean horizontal and vertical brightness temperatures are computed separately for both sensors for each grid cell. For each grid point of the SMOS ISEA 4H9 grid we compute the daily SMOS TBs using the 40° fit. Then the brightness temperatures are regridded to the NSIDC 12.5 km grid commonly used for sea ice maps. SMAP brightness temperature data are gridded directly to the NSIDC grid using a Gaussian resampling. The two resulting TB datasets are averaged. Finally the
10 sea ice thickness retrieval for 40° incidence angle is applied. The result is a SIT map that has the benefit of using data from both sensors (Fig. 5 (left)): it has a larger coverage, and is less affected by RFI sources. Also due to the 12 hours difference in the equator crossing time between the two sensors, the combined brightness temperatures are more representative for a daily mean. The RMSD between the original 40° to 50° incidence angle daily mean retrieval from Sect. 3.1 and the new mixed sensor one is 2.14 cm for the three months period investigated, while the bias is -0.63 cm (see also Fig. 5 for an example of the
15 spatial distribution of differences on 11 October 2015).

5 Conclusions

The original validated SMOS thin sea ice thickness algorithm from Huntemann et al. (2014) has been adapted to SMAP data. The existing retrieval for thickness of thin sea ice from the L-band sensor SMOS (launched 2009) has been adapted to SMAP (launched 2015) by (i) modifying the SMOS retrieval to use 40° incidence angle instead of the average in the range 40° to 50°,
20 (ii) establishing a linear regression between the SMOS and SMAP brightness temperatures at 40° incidence angle.

To derive the SMOS brightness temperature at 40° incidence angle required for the first step, an analytical function is fitted to the incidence angle dependent brightness temperatures. Using SMAP data and the SMOS data fitted to the same incidence angle to calibrate the SMAP TBs to those of SMOS has improved the TB RMSD between the two datasets for both polarizations with 2.7 K and 2.81 K for TB_h and TB_v , respectively. This is an improvement from previous attempts (Huntemann et al., 2016)
25 where the the RMSD for both polarizations was over 4 K showing that using fixed incidence angles for SMOS data increases the accuracy. Moreover the SMOS based retrieval has been adjusted for the new SMOS data version 6.20. The new algorithm contains a new RFI filtering routine exploiting the dependence of the brightness temperatures on the incidence angle. This results in improved coverage for RFI affected areas.

Concluding, the benefit of SMAP for retrieval of thickness of thin sea ice is twofold: first, the combined product has the
30 advantage of better spatial and temporal coverage that in future studies can allow insights on a sub-daily scale. Second, SIT can be retrieved from SMAP data alone, with similar accuracy as with SMOS, making the production chain more stable in the



case of malfunction of one of the two sensors. A full validation of the current retrieval requires a comparison with independent in-situ sea ice thickness data.

Data availability. <https://seaice.uni-bremen.de> (will shortly be available)

Competing interests. No competing interests are present

- 5 *Acknowledgements.* We gratefully acknowledge the support from the Transregional Collaborative Research Center (TR 172). "Arctic Amplification: Climate Relevant Atmospheric and Surface Processes, and Feedback mechanisms (AC)3" funded by the German Research Foundation (DFG, Deutsche Forschungsgemeinschaft).



References

- Bilello, M. A.: Formation, growth, and decay of sea-ice in the Canadian Arctic Archipelago, *Arctic*, 14, 2–24, 1961.
- Castro, R.: Analytical Pixel Footprint, Technical note, available at: <http://smos.com.pt/downloads/release/documents/so-tn-dme-11pp-0172-analytical-pixel-footprint.pdf> (last access: 6 April 2017), 2008.
- 5 Huntemann, M. and Heygster, G.: A New Method to Filter Out Radio-Frequency Interference (RFI) from SMOS Level 1C Data for Sea Ice Applications, in: *Towards an Interdisciplinary Approach in Earth System Science*, edited by Lohmann, G., Meggers, H., Unnithan, V., Wolf-Gladrow, D., Notholt, J., and Bracher, A., pp. 91–98, Springer International Publishing Switzerland, 2015.
- Huntemann, M., Heygster, G., Kaleschke, L., Krumpfen, T., Makynen, M., and Drusch, M.: Empirical sea ice thickness retrieval during the freeze-up period from SMOS high incident angle observations, *The Cryosphere*, 8, 439–451, 2014.
- 10 Huntemann, M., Patilea, C., and Heygster, G.: Thickness of thin sea ice retrieved from SMOS and SMAP, in: *Proceedings of 2016 IEEE International Geoscience and Remote Sensing Symposium (IGARSS)*, pp. 5248–5251, 2016.
- Indra Sistemas S.A.: SMOS Level 1 and Auxiliary Data Products Specifications, Product Document, Madrid, 2015.
- Kaleschke, L., Maaß, N., Haas, C., Hendricks, S., Heygster, G., and Tonboe, R. T.: A sea-ice thickness retrieval model for 1.4 GHz radiometry and application to airborne measurements over low salinity sea-ice, *The Cryosphere*, 4, 583–592, 2010.
- 15 Kaleschke, L., Tian-Kunze, X., Maaß, N., Mäkynen, M., and Drusch, M.: Sea ice thickness retrieval from SMOS brightness temperatures during the Arctic freeze-up period, *Geophysical Research Letters*, 39, 105501, 2012.
- Kerr, Y. H., Waldteufel, P., Wigneron, J. P., Martinuzzi, J., Font, J., and Berger, M.: Soil moisture retrieval from space: the Soil Moisture and Ocean Salinity (SMOS) mission, *IEEE Transactions on Geoscience and Remote Sensing*, 39, 1729–1735, 2001.
- Lannoy, G. J. M. D., Reichle, R. H., Peng, J., Kerr, Y., Castro, R., Kim, E. J., and Liu, Q.: Converting Between SMOS and SMAP Level-1
20 Brightness Temperature Observations Over Nonfrozen Land, *IEEE Geoscience and Remote Sensing Letters*, 12, 1908–1912, 2015.
- Sahr, K., White, D., and Kimerling, A. J.: Geodesic Discrete Global Grid Systems, *Cartography and Geographic Information Science*, 30, 121–134, 2003.
- SMOS Calibration team and Expert Support Laboratory Level 1: SMOS L1OPv620 release note, Release Note, ESA, 2015.
- Tian-Kunze, X., Kaleschke, L., Maaß, N., Mäkynen, M., Serra, N., Drusch, M., and Krumpfen, T.: SMOS-derived thin sea ice thickness:
25 algorithm baseline, product specifications and initial verification, *The Cryosphere*, 8, 997–1018, 2014.
- Zhao, T. J., Shi, J. C., Bindlish, R., Jackson, T. J., Kerr, Y., Cosh, M. H., Cui, Q., Li, Y. Q., Xiong, C., and Che, T.: Refinement of SMOS multiangular brightness temperature toward soil moisture retrieval and its analysis over reference targets, *IEEE Journal of Selected Topics in Applied Earth Observations and Remote Sensing*, 8, 589–603, 2015.
- Zine, S., Boutin, J., Font, J., Reul, N., Waldteufel, P., Gabarro, C., Tenerelli, J., Petitcolin, F., Talone, J. V. M., and Delwart, S.: Overview of
30 the SMOS sea surface salinity prototype processor, *IEEE-Transactions on Geoscience and Remote Sensing*, 46, 621–645, 2008.

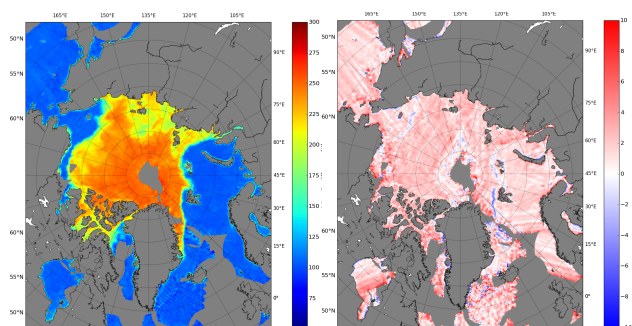


Figure 1. SMOS intensity for 6.20 data (left) for 29 October 2010 ; Intensity difference (right) between the 6.20 and the 5.05 data versions.

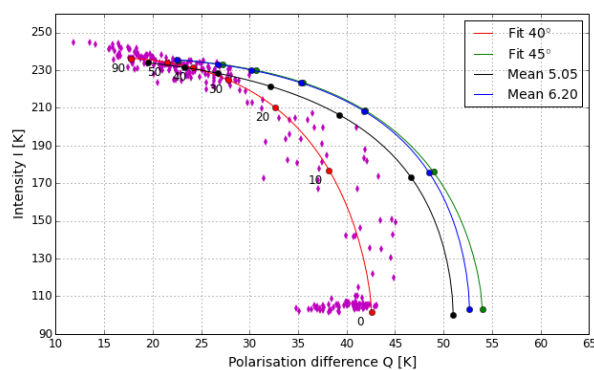


Figure 2. Sea Ice Thickness retrieval curves derived from SMOS data representing original algorithm (black), new data version (blue), 45° (green) and 40° (red) incidence angle fitted brightness temperatures. Dots represent data from the three training areas used for obtaining the 40° fit curve. Numbers under the curve represent the SIT in centimeters.

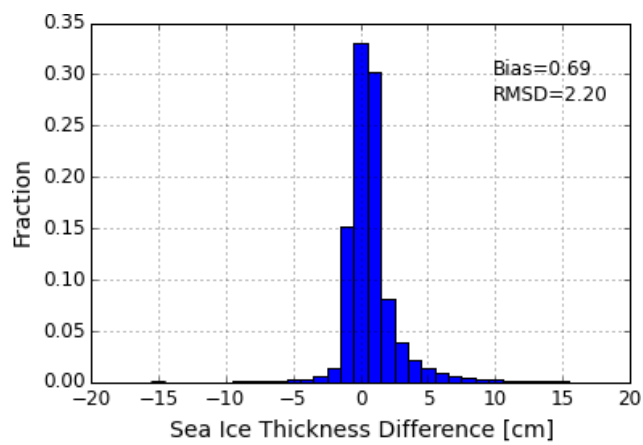


Figure 3. Histogram of SMOS sea ice thickness difference between daily mean retrieval and 45° incidence angle fitted brightness temperatures retrieval on 29 October 2010.

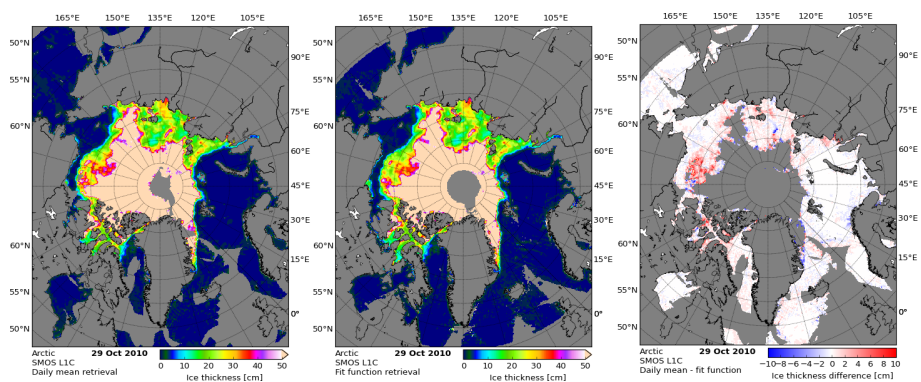


Figure 4. SMOS sea ice thickness retrieved on 29 October 2010 using 6.20 retrieval (left), retrieval using 45° incidence angle fitted brightness temperatures (central), and the difference between the two (right) with areas over 50 cm SIT not shown.

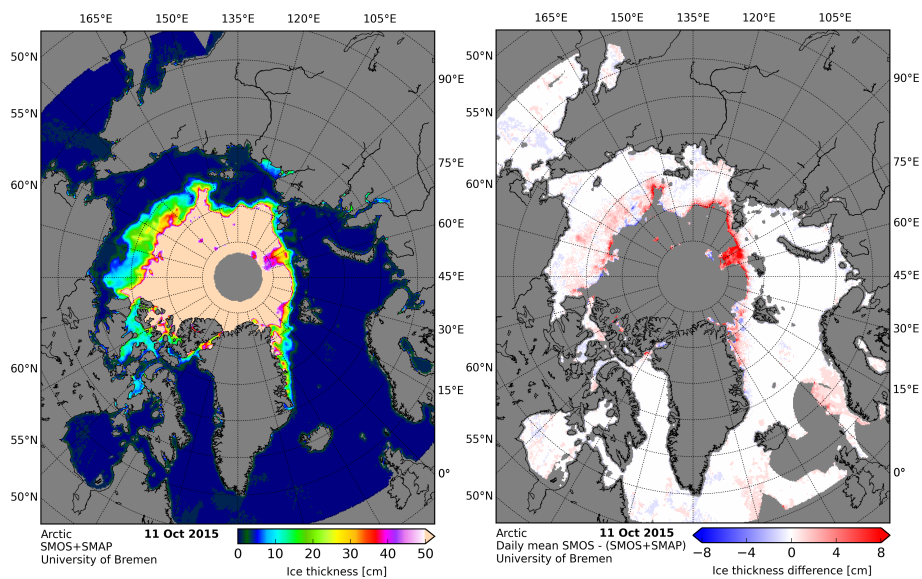


Figure 5. Sea Ice Thickness retrieved on 11 October 2015 for the joint SMOS+SMAP product (left) and the SIT difference between the SMOS daily mean retrieval and the joint product (right)



Table 1. Sea ice thickness retrieval curve parameters for the original 5.05 data version training, 6.20 training, and the two fit curve parameters for 40° and 45° incidence angle

Retrieval	Parameter	a [K]	b [K]	c [cm]	d
5.05	I_{abc}	100.2	234.1	12.7	-
	Q_{abcd}	51.0	19.4	31.8	1.65
6.20	I_{abc}	103.0	235.7	12.7	-
	Q_{abcd}	52.7	22.3	33.2	1.60
fit 40°	I_{abc}	101.5	236.4	12.2	-
	Q_{abcd}	42.6	17.3	32.9	1.39
fit 45°	I_{abc}	103.3	235.4	12.5	-
	Q_{abcd}	54.0	22.2	33.0	1.47



Table 2. Parameters for linear regression between SMOS and SMAP brightness temperatures

Polarization	Slope	Intercept [K]	RMSD [K]	r
<i>H</i>	0.996	3.68	2.70	0.999
<i>V</i>	0.985	7.03	2.81	0.997